

Ab Initio Modeling of the Metal–Support Interface: The Interaction of Ni, Pd, and Pt on MgO(100)

Núria López and Francesc Illas*

Departament de Química Física, Facultat de Química, Universitat de Barcelona, C/Martí i Franqués 1, 08028 Barcelona, Spain

Received: August 12, 1997; In Final Form: November 19, 1997

The interaction of Ni, Pd, and Pt on MgO has been investigated using cluster models and a variety of ab initio techniques. The case of a single Pd atom with acidic and basic sites of the MgO(100) surface has been chosen to test the adequacy of different ab initio wave functions and DFT techniques. Both approaches result in a similar description but only if large basis sets, including high angular momentum terms, and extensive treatment of the many-body effects are accounted for in the ab initio cluster model wave function. The DFT results appear to be more stable and less dependent on the basis sets. When properly compared, both approaches lead to the same conclusion. Pd interacts in a rather weak way with the acidic sites, but a moderately large interaction is predicted for interaction above the basic sites. Next, the interaction of Ni, Pd, and Pt on the basic sites of the MgO(100) surface is considered. The general trend is that the interaction energy increases from Ni to Pt. The nature of the bond is rationalized by analysis of the dipole moment curves and of the molecular orbitals.

I. Introduction

Deposition of transition-metal atoms on a variety of substrates is a common way to prepare a broad class of heterogeneous catalysts known as supported metal catalysts.¹ In these systems, the substrate used is an ionic material and, among current supports, metal oxides are widely employed.^{1,2} The support is supposed to have no influence on the catalytical reaction and to act as a passive spectator on top of which metal clusters, with well-defined catalytical activity, grow. However, the role of the support in the catalytical reaction is not always as inert as initially thought. In some cases the metal support interaction is so important that it has been generally termed strong metal support interactions, SMSI.^{3,4} A detailed understanding of the chemical nature of the metal–oxide interaction may be obtained by means of surface science experimental techniques applied to the metal–oxide interface.² However, the complexity of these systems makes it difficult to obtain direct, structural or electronic, information even under ultrahigh-vacuum, well-defined, controlled, experimental conditions. The interpretation of the experimental data for metal–support interfaces requires, no doubt, the use of quantum mechanical models. However, ab initio theoretical studies in this direction have been started only quite recently.

The relatively scarce theoretical information on the nature of the metal–support interaction does not yet permit a unified picture of these complex chemical systems. Among the few theoretical works dealing with the metal–support interaction we quote the Hartree–Fock calculations for the interaction of Ti on MgCl₂, described by Lin and Catlow,⁵ and of Cu on MgO(100), reported by Bacalis and Kunz.⁶ For the latter, the Hartree–Fock calculations are able to predict only a very weak, almost repulsive, interaction. This Hartree–Fock weak interaction contrasts with the moderate to large one predicted by calculations carried out on the framework of density functional

theory within the LDA, or local density approximation.⁷ In fact, more recent studies on the Cu/MgO(100) interface carried out by means of the generalized gradient corrected,⁸ GGA, and, also, of Hartree–Fock plus Moller–Plesset second-order perturbation theory⁹ show a very similar picture of the chemical bonding which is described as a weak interaction but not as weak as that previously reported by purely Hartree–Fock calculations.⁶ These first studies point out the importance of electronic correlation in the description of the metal–support chemical bond. In fact, electronic correlation effects must be explicitly included to be able to describe, even in a qualitative way, the nature of the metal–support interaction.

From a theoretical point of view, a systematic study is needed to achieve a deeper understanding of the nature of the metal–support interaction. Hence, it is desirable to have more studies on the same metal varying the support, and on the same support but with different metals. In a recent paper, a systematic study on the interaction of transition metals with the MgO(100) surface has been reported.¹⁰ These authors show that some of the selected transition metals interact strongly with this metal oxide surface while others, like Cu, only show a weak interaction. The ab initio study reported by Yudanov et al.¹⁰ relies entirely on the use of a DFT-GGA approach. Given the unusual chemical interactions that are present on the metal–support interface, it seems necessary to validate the DFT calculations against accurate, well-defined, ab initio wave function based methods. This is precisely one of the goals of the present theoretical study. To this end, we have chosen the Pd/MgO(100) system because of the available experimental information^{11,12} and, also, of the recent Hartree–Fock cluster model¹³ and DFT cluster¹⁰ and periodic¹⁴ calculations. This initial study permits us to define a proper computational scheme, which is then applied to study the interaction of Ni, Pd, and Pt above the basic centers of MgO(100).

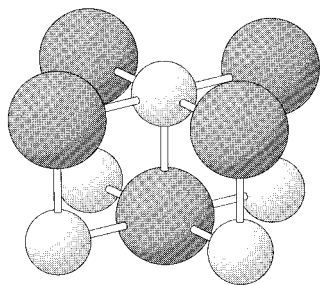


Figure 1. Schematic representation of the Mg_5O_5 cluster model used to represent the acid sites of the $\text{MgO}(100)$ surface. Large spheres represent anions, and smaller spheres, cations.

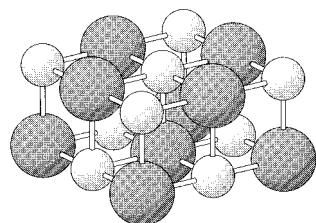


Figure 2. Schematic representation of the Mg_9O_9 cluster model used to represent the acid sites of the $\text{MgO}(100)$ surface. Large spheres represent anions, and smaller spheres, cations.

II. Surface Cluster Models

Different surface cluster models have been used to represent acidic, cationic and basic, anionic centers of the ideal, unreconstructed, $\text{MgO}(100)$ surface. The surface cluster models have been chosen in such a way that the stoichiometry of MgO is retained. Thus, Mg_5O_5 and Mg_9O_9 are selected to simulate the acidic sites where a metal atom will interact directly above a Mg^{2+} cation. These clusters contain two layers of ions and are further embedded in a suitable environment. The Mg_5O_5 cluster (Figure 1) contains one cation and four anions in the first layer and one anion and four cations in the second one. Similarly, the first layer of the Mg_9O_9 cluster (Figure 2) contains five cations and four anions, whereas the second layer contains four cations and five anions, thus representing the logical extension of the Mg_5O_5 cluster by addition of the second neighbor ions shell. The surface basic sites are those where the metal interacts above an O^{2-} anion and are represented by O_5Mg_5 and O_9Mg_9 clusters, which, before including the embedding scheme, are just the same for the cationic sites but upside down.

Since MgO is a largely ionic system,^{15–20} it is necessary to include the long-range Madelung potential. In fact, recent work has shown that while the Madelung potential develops quite rapidly even for moderately large clusters, considerable errors can arise from models that do not explicitly account for the Madelung field.²¹ Therefore, the present Mg_5O_5 , Mg_9O_9 , O_5Mg_5 , and O_9Mg_9 clusters have been embedded in an array of $13 \times 13 \times 4$ point charges. The magnitude of the point charges used to account for the Madelung potential is that corresponding to the bulk material, i.e., ± 2.0 . As shown recently, the ionicity of the bulk and regular surface sites does not exhibit substantial differences.²² The surface cluster models that explicitly include the point charge array will be denoted as $\text{Mg}_5\text{O}_5+\text{PCs}$, $\text{Mg}_9\text{O}_9+\text{PCs}$, $\text{O}_5\text{Mg}_5+\text{PCs}$, and $\text{O}_9\text{Mg}_9+\text{PCs}$, respectively.

The introduction of the point charge array, though necessary to properly account for long-range electrostatic effects, can further produce undesired artifacts.²³ In fact, the $+2.0$ point charges surrounding the edge O^{2-} anions will induce a large,

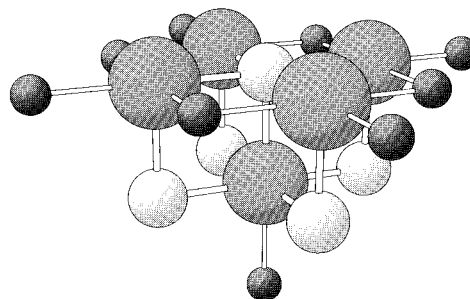


Figure 3. Schematic representation of the $\text{Mg}_5\text{O}_5 + \text{TIPs}$ cluster model used to represent the acid sites of the $\text{MgO}(100)$ surface. Large spheres represent anions; smaller spheres, cations; and dark small spheres, the cations represented by TIPs.

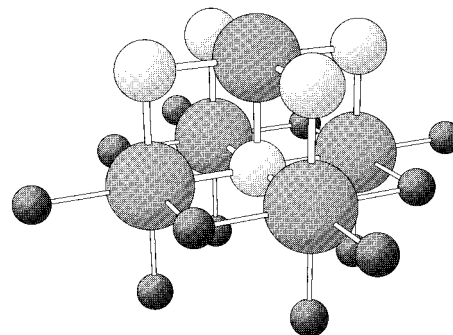


Figure 4. Schematic representation of the O_5Mg_5 cluster model used to represent the acid sites of the $\text{MgO}(100)$ surface. Large spheres represent anions; smaller spheres, cations; and dark small spheres, the cations represented by TIPs.

artificial, polarization of their electronic density toward the point charge. Several procedures^{24–27} have been proposed to avoid this artificial polarization. All these procedures share a common feature, namely, to explicitly include the finite ion size of those ions that surround the cluster atomic centers and are only represented by PCs in the clusters described above. The explicit inclusion of the finite ion size for the PCs in the edge allows us to exclude the electron density from this region and to avoid the artificial polarization described above. Among the different procedures available in the literature, the one suggested by Winter et al.²⁸ has been chosen. This approach is convenient because it simply adds a pseudopotential to the point charges representing the cations surrounding the edge anions. The combination of the point charge and the pseudopotential leads to a total ion potential, TIP, which includes the Madelung field but avoids artificial polarization. The effect of the TIPs has been investigated in the smaller cluster models only. The cluster models that include both TIPs and PCs are denoted as $\text{Mg}_5\text{O}_5+\text{TIPs}+\text{PCs}$ and $\text{O}_5\text{Mg}_5+\text{TIPs}+\text{PCs}$. (See Figures 3 and 4).

Finally, we would like to add some brief comments on the use of nonstoichiometric clusters. For MgO it is always possible to choose a cluster that retains the bulk stoichiometry. However, for other materials it is not easy, or not convenient at all, to design such a cluster, and it is customary to use nonstoichiometric clusters that are “charged” in the sense that the number of electrons included is that of the formally ionic material, although the embedding procedure leads, of course, to an overall neutral model. Examples of “charged” clusters are $[\text{NiO}_6]^{8-}$ used to investigate the ligand field splitting and optical spectrum of $\text{NiO}^{29–36}$ or $[\text{Ni}_2\text{F}_{11}]^{7-}$, $[\text{Ni}_2\text{O}_{11}]^{18-}$, or $[\text{Cu}_2\text{O}_{11}]^{20-}$ used to investigate the origin of magnetic coupling in KNiF_3 , K_2NiF_4 , NiO , or La_2CuO_4 .^{37–40} In addition to the stoichiometric clusters described above, we have also used a $[\text{MgO}_5]^{8-} + \text{TIPs} + \text{PCs}$

to study the interaction of Pd above the cationic site of MgO. Results for this nonstoichiometric cluster are, not surprisingly, identical to those found for the stoichiometric clusters described above and, hence, will not be further described.

III. Computational Approach

The electronic structure of the MgO surface cluster models used in this work is fairly simple since the constituent ions are all closed shell diamagnetic centers, the resulting electronic configuration being always a closed shell. However, the electronic structure of the Ni, Pd, and Pt metal atoms is complicated because of the closeness between the different low lying electronic configurations with different md shells ($m = 3, 4, 5$ for Ni, Pd, Pt) occupation: md^n , $md^{n-1}(m+1)s^1$, $md^{n-2}(m+1)s^2$. The ground state of Ni (and Pt) is a 3D with $3d^9 4s^1$ ($5d^9 6s^1$) configurations, whereas Pd has a $4d^{10}$ (1S) ground state. The energy difference between the ground and first excited state for Ni (3D from $3d^8 4s^2$), Pd (3D from $4d^9 5s^1$), and Pt (1S from $4d^{10}$) is 0.03, 0.95, and 0.48 eV, where an average of the energy levels derived from the spin-orbit splitting of a given multiplet has been considered when necessary.⁴¹ The need to explicitly account for the mixing between these md^n , $md^{n-1}(m+1)s^1$ and $md^{n-2}(m+1)s^2$ configurations adds further appeal for theoretical study and already points out the importance of electronic correlation effects. However, the case of Pd is special because of the closed-shell nature of the ground state of both, metal and cluster model, interacting fragments. This fact enables us to start with a single Hartree-Fock reference determinant and explore different theoretical approaches.

The overall set of calculations reported in this work has been carried out using relatively large basis sets. For Ni, Pd, and Pt, the small core, 18-electron, relativistic, pseudopotential of Hay and Wadt⁴² has been employed together with the uncontracted set of primitive GTOs with exponents taken from ref 42. The metal basis sets have 5s, 5p, and 5d for Ni, 5s, 5p, and 4d for Pd, and 5s, 5p, and 3d for Pt. For MgO, we explicitly consider all its electrons by using different sets of contracted Gaussian type orbitals, CGTOs, depending on the cluster model employed. Two different basis sets are used for cations of the simplest Mg_5O_5 cluster model. For the atop Mg^{2+} in the basis set it is necessary to include a good representation of the 3s and 3p orbital. This is accomplished by taking the [13s,8p/6s,3p] set used by Pacchioni et al. to study the influence of the Madelung field in the chemisorption of various species on $MgO(100)$.²¹ The remaining cations of Mg_5O_5 are not directly involved in the interaction with Pd and can be described by a smaller, [12s,7p/5s,2p], basis set taken also from ref 21. To describe the O^{2-} anions of the Mg_5O_5 and O_5Mg_5 clusters, we tested two different basis sets, both optimized to accurately describe O^- . These two basis sets are the [9s,5p/4s,3p] one, with exponents and contraction coefficients taken from Broughton and Bagus,⁴³ and the [8s,4p/4s,2p] double- ζ basis set of Huzinaga.⁴⁴ Hereafter, these two basis sets will be referred to as Basis-1 and Basis-2, respectively. For the O_5Mg_5 model the [13s,8p/6s,3p] basis set was chosen to describe the Mg^{2+} cations. The larger Mg_9O_9 and O_9Mg_9 models have been built up by extending the former cationic and anionic models and using Basis-2 for all the O^{2-} , whereas the outermost Mg^{2+} cations in the second layer are described with a more, [7s,4p/2s,1p], contracted set taken also from Huzinaga.⁴⁴

Using the basis sets described above, the potential energy curves for the interaction of Pd with each one of the cluster models described above have been calculated at various levels of theory. First, a variety of ab initio wave function based

methods were used; these include Hartree-Fock and second-order Moller-Plesset, MP2, perturbation theory. Results from these ab initio techniques were later compared to those obtained from a density functional theory, DFT, approach in which the gradient-corrected Becke⁴⁵ exchange and Lee-Yang-Parr⁴⁶ correlation functional, based on the original work of Colle-Salvetti on the He atom,⁴⁷ were used. As usual, the resulting functional is referred to as BLYP. All wave function based and DFT calculations were carried out using the same basis sets and pseudopotentials. More accurate calculations on key systems were also carried out to gain further understanding of the nature of the interaction and to identify the bonding mechanisms. These more extended calculations include higher order of perturbation theory, MP3 and MP4, and coupled cluster techniques such as coupled cluster with double excitations, CCD, with single and double excitations, CCSD, and with the correction for the triple excitations, CCSD(T). To ameliorate the description of electronic correlation, the MP2 to MP4, CCD, CCSD, and CCSD(T) were repeated after adding f orbitals to the Pd basis set ($+f_{Pd}$) and d polarization functions to the O anion ($+d_O$) directly interacting with Pd. The exponent for the Pd f function was taken from Balasubramanian⁴⁸ and that of O from Siegbahn and Roos.⁴⁹ Results from these more accurate wave function calculations, which employ the extended basis sets, have also been compared with those arising from density functional, within the BLYP approach. Finally, results will be presented for the B3LYP hybrid method, which combines the Becke three-parameter exchange functional⁵⁰ and the LYP correlation one. To avoid an unnecessary and excessive amount of information, the B3LYP calculations for this case will be reported for some selected systems only.

The calibration calculations for Pd on MgO permit establishing the adequacy of the BLYP or B3LYP approaches. These calculations also show that the relevant interaction takes place above the basic sites. Therefore, the comparative study of Ni, Pd, and Pt on $MgO(100)$ has been carried out at the B3LYP level and for the basic sites only.

Finally, we must mention that although the basis sets used in this work are reasonably large so as to have confidence in the calculated results, they are not free of basis set superposition error, BSSE. Therefore, all computed potential energy curves have been corrected using the standard counterpoise method of Boys and Bernardi⁵¹ to avoid BSSE.

All calculations have been carried out using the Gaussian-94 suit of programs.⁵²

IV. Calibration Calculations for Pd on $MgO(100)$

Before starting this section, we would like to point out the critical importance of the oxygen basis set. This does affect directly the interaction on the acidic sites because the surface cluster models for this site contain not less than four surface oxide anions. A very stringent test for the quality of the O basis set in ionic systems is given by ΔT , the increment in the expectation value of the kinetic energy when going from the gas-phase atom to the O^{2-} ion in the crystal. We have computed these values by using a model for the bulk consisting of a single oxygen anion surrounded by 6 TIPs and 336 optimized PCs. In Table 1, we compare ΔT from Basis-2 with previous values using Slater type orbitals, STO, and different kinds of embedding schemes. It is important to realize that Basis-2, being optimized in O^- , provides a good description for the anion in the bulk. Its quality is comparable to the the 5s5p STO set used by Luaña, Recio, and Pueyo in their ab initio perturbed ion study of bulk MgO ⁵³ and significantly better than the results that are obtained

TABLE 1: Increment of Kinetic Energy, $\Delta T = \langle T \rangle_{\text{ion}} - \langle T \rangle_{\text{atom}}$, in eV, for Oxygen in Bulk MgO as Obtained in the Present Work and Compared with Previous Available Results (for a Detailed Discussion See Ref 49)

calculation	basis	ΔT
experimental estimate for MgO		+32.9
free ion	ref 49 5s4p STOs	-7.61
Watson sphere	ref 49 4s4p STOs	-3.60
Pandey and Vail	ref 49 7s4p STOs	+10.05
Luaña, Recio, and Pueyo	ref 49 5s5p STOs	+28.76
Basis-2	present work (8s4p/4s2p) GTO	+25.92
near HF	present work 18s13p GTO	+16.36

TABLE 2: Equilibrium Distances, r_e in au, Dissociation Energies, D_e in eV, and Vibrational Frequencies, ω_e in cm^{-1} , for the Adsorption of Pd on the Cationic Sites Modeled by Different Clusters Embedded in the Point Charge Array

O basis set		Basis-1 Mg ₅ O ₅ +PCs	Basis-2 Mg ₅ O ₅ +PCs	Basis-2 Mg ₉ O ₉ +PCs
SCF	r_e	5.95	6.00	5.99
	D_e	0.03	0.02	0.02
	ω_e	23	29	31
MP2	r_e	5.60	5.67	5.66
	D_e	0.11	0.08	0.09
	ω_e	42	38	38
BLYP	r_e	5.17	5.14	5.12
	D_e	0.28	0.24	0.26
	ω_e	76	76	78

using the near-Hartree–Fock basis optimized by Partridge for neutral oxygen.⁵⁴ These preliminary results illustrate the adequacy of the present approach, basis sets, and embedding scheme, to represent MgO in a condensed-phase environment.

(a) Interaction of Pd on Acidic Sites of MgO(100). The interaction of Pd on the acidic sites of MgO(100), modeled by the Mg₅O₅ and Mg₉O₉ clusters, predicted by the different computational methods is qualitatively similar. Moreover, the results for different cluster sizes using the same basis set, Mg₅O₅ and Mg₉O₉ with Basis-2, and for a given cluster model with two basis sets, Mg₅O₅ with Basis-1 and Basis-2, are quite close, indicating that the results are quite stable with respect to either basis set and cluster size (See Table 2). On this site, bonding of atomic Pd to MgO(100) is always predicted to be very weak, especially at the Hartree–Fock, SCF, level. Introduction of correlation effects by means of MP2 leads to a slightly stronger interaction and quite shorter distances. However, DFT results for the interaction energies, within the BLYP exchange–correlation functional, are almost twice the MP2 value. Given the fact that the interaction is in all cases very weak, this fact does not seem to be especially relevant. We must mention that the present BLYP results are in agreement with those reported by Yudanov et al.¹⁰

Now, let us consider the effect of embedding the Mg₅O₅ cluster model on TIPs and PCs as opposite the previous results where only PCs were considered. The fact that no spectacular changes appear when going from Mg₅O₅ to Mg₉O₉ already indicates that one should not expect large differences by adding TIPs to the Mg₅O₅ model. Results in Table 3 show that this is indeed the case. The only noticeable difference appears for the SCF calculations where the interactions becomes almost negligible, with the potential curve exhibiting a repulsive character. The fact that the TIPs do not largely affect the results which explicitly include electronic correlation is consistent with the contracted character of the Mg²⁺ cations. The edge anions will be polarized toward their nearest neighbor positive point charges, but this does not affect the compact electronic cloud, almost corelike, of the atop cation.

TABLE 3: Effect of the Embedding on the Interaction of Pd on Mg₅O₅+PCs Clusters (Basis-2 Has Been Employed for Oxygens): Units Are as in Table 1

method	PCs ^a			TIPs+PCs ^b		
	r_e	D_e	ω_e	r_e	D_e	ω_e
SCF	6.00	0.02	30			
MP2	5.67	0.08	38	5.83	0.04	29
BLYP	5.14	0.24	76	5.07	0.30	81
B3LYP	5.15	0.20	72	5.11	0.22	71

^a Point charge embedding. ^b Mixed embedded scheme as described in section II.

TABLE 4: Equilibrium Distances, r_e in au, Dissociation Energies, D_e in eV, and Vibrational Frequencies, ω_e in cm^{-1} , for the Adsorption of Pd on the Anionic Sites Modeled by Different Clusters Embedded in the Point Charge Array

O basis set		Basis-1 O ₅ Mg ₅ +PCs	Basis-2 O ₅ Mg ₅ +PCs	Basis-2 O ₉ Mg ₉ +PCs
SCF	r_e	4.89	4.89	5.17
	D_e	0.05	0.05	0.03
	ω_e	42	43	29
MP2	r_e	4.33	4.33	4.36
	D_e	0.33	0.32	0.31
	ω_e	96	97	93
BLYP	r_e	4.09	4.02	4.04
	D_e	0.72	0.79	0.74
	ω_e	138	159	155

To further investigate the dependence of the DFT techniques on the exchange–correlation potential, we report in Table 3 results obtained using the nowadays worldwide famous B3LYP hybrid functional. Both BLYP and B3LYP functionals lead to quite the same results. Although the definition of exchange and correlation in wave function based methods does not have a one-to-one correspondence with that of DFT, one is tempted to relate the closeness of BLYP and B3LYP results with the fact that, according to wave function based results, the bonding mechanism is basically due to correlation effects.

(b) Interaction of Pd on Basic Sites of MgO(100). The interaction of Pd with the anionic, O²⁻, sites of the MgO surface is quite different than on the acidic sites and presents some particular features. Before entering into these specific peculiarities, we would like to point out that, as for the interaction on the acidic site, results for O₅Mg₅ within Basis-1 and Basis-2 are quite similar and that not noticeable changes are introduced when going from O₅Mg₅ to the larger O₉Mg₉ cluster. Now, we note first that, except for the Hartree–Fock results, the interaction energy is much larger than for the acidic sites. At first sight the BLYP results are quite curious because they are about twice as large as the MP2 values (Table 4). This was already observed for the acidic site but there the interaction energy was very small so that doubling a value did not have the significance as here. Consistently with a stronger interaction, the BLYP values for the equilibrium distance and vibrational frequency for the mode perpendicular to the surface are shorter and larger than the MP2 values, respectively.

Next, we analyze the effect of the embedding method used to represent the remaining crystal. At variance with the acidic site, results for the interaction above a basic site are considerably affected by the presence of the TIPs. The interaction energies are enhanced by about 20%, and the difference between MP2 and DFT, BLYP, or B3LYP, results increases considerably although the relative effect is the same; the DFT results are again about twice the MP2 ones. The introduction of the TIPs leads to a stronger bond and, consequently, to shorter distances and larger frequencies. The fact that the effect of the TIPs is so large seems to be contrary to the fact that results for O₅Mg₅

TABLE 5: Effect of the Embedding on the Interaction of Pd on O₅Mg₅ Clusters (Basis-2 Has Been Employed for Oxygens): Units Are Those of Table 1

method	PCs ^a			TIPs+PCs ^b		
	<i>r_e</i>	<i>D_e</i>	<i>ω_e</i>	<i>r_e</i>	<i>D_e</i>	<i>ω_e</i>
SCF	4.89	0.05	43	4.68	0.12	60
MP2	4.33	0.32	97	4.25	0.49	111
BLYP	4.02	0.79	159	4.00	1.08	166
B3LYP	4.04	0.65	149	4.02	0.89	160

^a Point charge embedding. ^b Mixed embedded scheme.

and O₉Mg₉ are almost identical. However, a deeper look at these surface cluster models shows that both clusters have anions at the cluster edge sites. These anions are polarized to the PCs and produce a decrease of electronic density at the surface site. The use of the TIPs prevents this artifact in a simple, yet efficient, way. Once again, we must point out that an identical effect of the TIPs for this site has been found by Rosch et al.⁵⁵

So far, the description of the interaction above the basic site resulting from MP2 and DFT approaches is qualitatively similar but the origin of the difference in the interaction energy remains unclear. Notice that depending on which value is taken, the interaction energy drops from ≈20 kcal/mol to barely 10 kcal/mol. In the first case one will describe the interaction as a rather strong chemisorption bond, whereas in the second case one will be tempted to describe the interaction as a dispersive one arising from intermolecular forces. Clearly, the origin of such difference must be addressed and solved. This will be the scope of the next subsection.

(c) Origin of the Difference between MP2 and DFT-GGA Results. The proper description of the interaction of metals on metal–oxide surfaces is an important issue in surface science and heterogeneous catalysis and merits a deeper understanding. Depending on the interaction energy between a metal and a support, different growth patterns will be predicted. It is therefore essential to be able to elucidate which of the theoretical treatments presented so far is adequate to describe this kind of interaction. To further investigate the origin of the difference between MP2 and BLYP results for the interaction of Pd on both acidic and basic sites, we have carried out single-point energy calculations at higher levels of theory and using the MP2 equilibrium distance of Pd above each site. The higher levels of theory include perturbation theory up to fourth order, MP3 and MP4, and coupled cluster calculations involving double excitations, CCD. These higher level calculations have been carried out for the clusters embedded in point charges only and also for those embedded in the TIPs and point charges. A summary of results is reported in Table 6.

For the cationic site there are no appreciable differences for the interaction energy computed at different levels, and one is tempted to claim that convergence on the perturbations series has been achieved. Interaction of Pd above the anionic sites is slightly more affected by the level of theory, but the interaction energy from MP2 to CCD only changes by about 0.06 eV and CCD and BLYP still differ by 0.4 eV! These results seem to add support to the convergence of the perturbation series. However, it is known that extensive inclusion of electronic correlation through configuration interaction or related techniques requires the inclusion of higher angular momentum functions to the basis set.^{56,57} We have therefore added an f function to the Pd set and a d polarization function to the atop oxygen of the O₅Mg₅ cluster model. The effect of each one of these functions has first been studied separately, but both polarization functions were later included in the calculations. In addition, we have also include the extended coupled cluster

TABLE 6: Interaction Energy of Pd above the Mg₅O₅+PCs, O₅Mg₅+PCs, Mg₅O₅+TIPs+PCs and O₅Mg₅+TIPs+PCs Cluster Models Computed from Single-Point Energy Calculations at Various Levels of Theory Carried Out at the MP2 Equilibrium Distance (Basis-2 Has Been Employed for Oxygens)

method	PCs		TIPs+PCs	
	<i>r</i>	<i>E_{int}</i>	<i>r</i>	<i>E_{int}</i>
Cationic Site				
MP2	5.67	0.08	5.83	0.04
MP3	5.67	0.08	5.83	0.04
MP4-DQ	5.67	0.08	5.83	0.04
CCD	5.67	0.08	5.83	0.04
BLYP	5.14	0.24	5.07	0.30
Anionic Site				
MP2	4.32	0.32	4.25	0.48
MP3	4.32	0.22	4.25	0.35
MP4-DQ	4.32	0.28	4.25	0.43
CCD	4.32	0.26	4.25	0.40
BLYP	4.02	0.79	4.00	1.08

TABLE 7: Interaction Energy, *E_{int}* in eV, from Single-Point Energy Calculations at Various Levels of Theory for the Anionic Site Described by O₅Mg₅+TIPs+PCs^a

<i>E_{int}</i>	<i>z_{Pd}</i> = 4.25 au				<i>z_{Pd}</i> = 4.02 au
	Basis-2	+d _O	+f _{Pd}	+d _O +f _{Pd}	+d _O +f _{Pd}
SCF	0.06	0.09	0.06	0.06	
MP2	0.48	0.50	0.65	0.69	0.78
MP3	0.35	0.37	0.49	0.51	0.57
MP4-DQ	0.43	0.44	0.55	0.57	0.64
CCD	0.40	0.42	0.53	0.56	
CCSD	0.49			0.70	0.71
CCSD(T)	0.56			0.79	0.80
BLYP	1.08				1.12
B3LYP	0.89				0.92

^a Calculations correspond to the MP2 (*z_{Pd}* = 4.25 au) and B3LYP (*z_{Pd}* = 4.02 au) equilibrium distance of Pd to the on top anionic site; +d_O stands for addition of a d function to the atop oxygen cluster atom, +f_{Pd} indicates that Pd basis includes an extra f function, and +d_O+f_{Pd} indicates that both d and f functions are included.

calculations by including explicitly the single excitations and the usual approximation for the triples. The CCSD(T) have been carried out for Basis-2 and the basis set that includes both Pd(f) and O(d). Since these are point calculations, the CCSD(T) ones have been repeated for the extended basis set at the B3LYP equilibrium distance so as to show their dependence on the distance. A summary of relevant results is given in Table 7.

The effect of polarization functions on the atop oxygen atom on the interaction energy is quite small, but that of the f function of Pd is important. This is quite surprising since one would expect a large effect of the f function on the electronic correlation of Pd, but one would not expect such large differential effects upon interaction with the surface model. The inclusion of a single f polarization function for Pd raises the interaction energy at the MP2 level by about 25%, with similar variations at the MP3, MP4 series and for CCD. Notice that at the SCF level the effect of this polarization function is almost zero, indicating the origin of a purely many-body effect in the interaction. This is consistent with the large role of single and triple excitations on the interaction energy. In fact, the CCSD and CCSD(T) calculations for Basis-2 and for Basis-2 + O_d + Pd_f were carried out at two equilibrium distances, those obtained at MP2–Basis-2 level and B3LYP–Basis-2 level of calculation. Results for Basis-2 already indicate the relevance of single and triple excitations that once again increase the interaction energy by an additional 25%. Finally, we consider the joint effect of the two polarization functions and of single and triple excitations

TABLE 8: Structural Parameters for the Interaction of Ni, Pd, and Pt on the Basic Site of MgO(100) As Obtained from B3LYP Calculations on a Metal–O₅Mg₅+TIPs+PCs Cluster Model^a

	Ni	Pd	Pt
r_e	3.50	4.02	3.86
$D_e(md^{10})$	2.23	0.89	2.19
D_e	0.70	0.89	1.53
ω_e	256	160	161
M_1	0.108	0.153	0.092
M_2	−0.139	−0.083	−0.041

^aDistances are in atomic units, frequencies in cm^{−1} and dissociation energies in eV; $D_e(md^{10})$ is the interaction energy with respect to the md^{10} configuration of each atom. M_1 and M_2 stand for the slope and curvature of the dipole moment curve at r_e .

on the coupled cluster wave function. As can be seen from results in Table 7, the inclusion of both basis set effects and single and triple excitations results in an interaction energy that is twice that calculated for the small basis and CCD calculations.

In principle, a proper comparison between DFT and ab initio wave functions should consider the same basis for both descriptions, although it has been suggested that the DFT techniques exhibit a reasonably rapid convergence with the angular expansions.⁵⁸ Nevertheless, we found it convenient to test the performance of the BLYP and B3LYP exchange–correlations functionals with respect the addition of d_0 and f_{Pd} higher angular momentum functions to Basis-2. Results show that, in fact, improvement on the basis set does not noticeably affect the DFT, BLYP, and B3LYP, results. Therefore, one must conclude that DFT can only be compared with highly accurate wave function based calculations. Surprisingly enough, the proper ab initio description of the interaction of a single Pd atom with surface cluster models of MgO(100) requires the use of large basis sets and sophisticated wave functions. However, an equally good description is obtained by means of the currently available DFT approaches.

The final calculated interaction energies are similar to those earlier reported by Yudanov et al.¹⁰ and are in good agreement with the experimental estimate of Henry et al.,⁵⁹ which is 0.7–1.0 eV. This is in agreement with the interaction energy computed for the interaction above the basic site.

V. Interaction of Ni, Pd, and Pt on the Basic Sites of MgO(100)

The systematic study described in the previous section shows that the B3LYP level is the DFT approach, whose results are closer to the ones obtained with the largest basis set and the most accurate wave function based method employed in this work, CCSD(T). Therefore, B3LYP appears to be appropriate to describe the interaction of Pd with acid and basic sites of MgO(100). We expect that B3LYP will provide a similar level of accuracy for all atoms in the same transition-metal triad. Here, we report a study of Ni, Pd and Pt with the basic sites of MgO(100), the only ones where a significant interaction occurs. First of all, we note that, in all cases, the electronic ground state of the supersystem is a closed-shell singlet. This is in agreement with previous work¹⁰ and is a first indication of a strong chemical interaction that completely quenches the magnetic behavior of isolated Ni and Pt. Results for the structural parameters of Ni, Pd and Pt above the basic site of MgO(100) are reported in Table 8.

At first sight, results follow the trend reported by Yudanov et al.¹⁰ even from a quantitative point of view. This is somehow surprising provided two different, BLYP and B3LYP, func-

tionals are used. The similarity of results extend to the analysis of the dipole moment curves, which provide information about the degree of charge transfer between two interacting systems.^{60,61} Of particular importance are the slope of the dipole moments and its curvature; large slopes and small curvatures are the fingerprint of ionic bonds, while small slopes and large curvatures are found when covalency is the dominant bonding effect. The slope of the dipole moment curve, at the equilibrium position, obtained from B3LYP is 0.11, 0.15, and 0.09 for Ni, Pd, and Pt, respectively, and the curvatures are ≈ 0.1 . This is a clear indication of a similar chemistry and of a small, if any, degree of charge transfer between the metal and the surface. These results are, again, similar to those described in ref 10 except for Ni, where we found a slope (0.11) smaller than the one (0.48) found in ref 10; this may be due to the fact that results in ref 10 for Ni are nonrelativistic, whereas relativistic ECPs are used here for all metal atoms. The present interaction energy for Ni on MgO(100) is also slightly different from that reported in ref 10. To understand the origin of this difference, we report in Table 8 the value obtained with respect to the md^{10} asymptote, which avoids any possible bias due to the treatment of the open-shell atomic reference.⁶² When comparing the present value with the one obtained using the data in ref 10, both with respect to the md^{10} asymptote, the difference persists. A possible explanation for the difference is the lack of relativistic effects for Ni in ref 10. However, introduction of relativistic effects often results in stronger interactions. Therefore, we should ascribe the difference to the use of a different exchange–correlation functionals despite the good agreement found for Pd and Pt. In any case, the physical description arising from either BLYP¹⁰ and present B3LYP exchange–correlation functionals is the same with minor differences for Ni only.

A point that merits additional discussion is the change in the atomic configuration for Ni and Pt upon adsorption. This change is easily explained if one considers the symmetry descent which permits the hybridization between the md_z^2 (z being the direction perpendicular to the surface) and the outermost “ $(m+1)s$ ” atomic orbital. One of the hybrid orbitals ($s+d_z^2$) concentrates electronic density above the surface more than the other ($s-d_z^2$). The latter is precisely the HOMO, whereas the former is the LUMO. This hybridization permits diminishing the Pauli repulsion between the O^{2−} and the “ $(m+1)s$ ” orbital, which has a rather large spatial extent opposite of the “ md ” one. This mechanism is also present in Pd, where the s – d hybridization also permits a decrease in the Pauli repulsion. Hence, the picture of the chemical bond is that of a polarized covalent bond where polarization or hybridization is the leading term simply because it permits decreasing the Pauli repulsion. This is in agreement with the analysis of the dipole moment curves described above. This interpretation allows us to explain why electronic correlation is so important when starting from a pure Hartree–Fock description. In fact, this hybridization mechanism also appears at the Hartree–Fock level, but its contribution is not taken into account properly because the excited multiplets lie too high in energy and the hybridization mechanism is much less efficient. Notice that this interpretation is possible only after a careful analysis of the Kohn–Sham orbitals and dipole moment curves for the whole triad.

VI. Conclusions

The nature of the interaction of Pd with acidic and basic sites of the MgO(100) surface has been investigated by ab initio wave functions and DFT techniques. Both approaches result in a similar description. However, this is true if, and only if, large

basis sets including high angular momentum terms and extensive treatment of the many-body effects are accounted for in the ab initio cluster model wave function. The DFT results do, however, appear to be more stable and less dependent on the basis sets. When properly compared, both approaches lead to the same conclusion. Pd interacts in a rather weak way with the acidic sites but a moderately large interaction is predicted for interaction above the basic sites.

The comparison between wave function and DFT approaches permits us to suggest that B3LYP is appropriate to study the interaction of Ni, Pd, and Pt on MgO(100). The B3LYP study on this series permits clarifying the origin of the bonding mechanism above the basic site, the only one where significant interaction occurs. From the ab initio wave function picture it is found that the interaction is built up from electronic correlation effects. However, combined use of B3LYP dipole moment curves and orbital analysis permits suggesting that the leading mechanism is s-d hybridization, which decreases the Pauli repulsion while maintaining the electrostatic attractive, charge-induced dipole terms. This interpretation in term of s-d hybridizations permits us to find an explanation for the crucial role of electronic correlation effects.

In conclusion, DFT techniques appear to be a promising tool for the study of the interaction of metals on ionic surfaces. Results for a complete series such as Ni, Pd, and Pt provided a rather detailed description of the bonding mechanism in these complex materials.

Acknowledgment. Part of this work was presented at the Symposium on Quantum Theory and Simulation of Bulk, Surface and Interface Phenomena held in Raleigh, June 17–18, 1997, and hosted by the North Carolina State University. The authors are indebted to all participants of this meeting for many stimulating discussions and suggestions. We are particularly indebted to Prof. Notker Rösch, Prof. Gianfranco Pacchioni, and Prof. Donald G. Truhlar. Financial support from the Spanish “Ministerio de Educación”, project DGICYT PB95-0847-CO2-01, partial support from “DGR de la Generalitat de Catalunya”, project 1995SGR-00048, and from NATO, CGR 941191, is fully acknowledged. Finally, the authors wish to thank the Fundació Catalana de la Recerca and C⁴ CESCA/CEPBA, for helping with the calculations.

References and Notes

- (1) Gates, B. C. *Chem. Rev.* **1995**, 95, 511.
- (2) Goodman, D. W. *Chem. Rev.* **1995**, 95, 523.
- (3) Tauster, S. J. *Acc. Chem. Res.* **1987**, 20, 389.
- (4) Tauster, S. J.; Fung S. C.; Garten, R. L. *J. Am. Chem. Soc.* **1978**, 100, 170.
- (5) Lin, J.S.; Catlow, C. R. A. *J. Catal.* **1995**, 157, 145.
- (6) Bacalis, N. C.; Kunz, A. B. *Phys. Rev. B* **1985**, 32, 4857.
- (7) Li, Y.; Langreth, D. C.; Pederson M. R. *Phys. Rev. B* **1995**, 52, 6067.
- (8) Pacchioni, G.; Rösch, N. *J. Chem. Phys.* **1996**, 104, 7329.
- (9) Lopez, N.; Illas, F. *J. Mol. Catal. A* **1997**, 119, 177.
- (10) Yudanov, I.; Pacchioni, G.; Neyman, K.; Rösch, N. *J. Phys. Chem. B* **1997**, 101, 2786.
- (11) Goyhenex, G.; Henry, C. R. *J. Electron Spectrosc. Relat. Phenom.* **1992**, 61, 65.
- (12) Chapon, C.; Henry, C. R.; Chemam, A. *Surf. Sci.* **1985**, 162, 747.
- (13) Ferrari, A. M.; Pacchioni, G. *J. Phys. Chem.* **1996**, 100, 9032.
- (14) Stirling, A.; Gunji, I.; Endou, A.; Oumi, Y.; Kubo, M.; Miyamoto, A. *J. Chem. Soc., Faraday Trans.* **1997**, 93, 1175.
- (15) Pacchioni, G.; Sousa, C.; Illas, F.; Parmigiani, F.; Bagus, P. S. *Phys. Rev. B* **1993**, 48, 11573.
- (16) Illas, F.; Lorda, A.; Rubio, J.; Torrance, J. B.; Bagus, P. S. *J. Chem. Phys.* **1993**, 99, 389.
- (17) Bagus, P. S.; Illas, F.; Sousa, C.; Pacchioni, G. In *Electronic Properties of Solids Using Cluster Methods*; Kaplan, T. A., Ed.; Fundamental Material Science I; Thorpe, M. F., Ed.; Plenum Press: New York, 1994.
- (18) Sousa, C.; Illas, F.; Bo, C.; Poblet, J. M. *Chem. Phys. Lett.* **1993**, 215, 97.
- (19) Casanovas, J.; Lorda, A.; Sousa, C.; Illas, F. *Int. J. Quantum Chem.* **1994**, 52, 281.
- (20) Pacchioni, G.; Illas, F. *Chem. Phys.* **1995**, 199, 155.
- (21) Pacchioni, G.; Ferrari, A. M.; Marquez, A. M.; Illas, F. *J. Comput. Chem.* **1997**, 18, 617.
- (22) Sousa, C.; Mejias, J. A.; Pacchioni, G.; Illas, F. *Chem. Phys. Lett.* **1996**, 249, 123.
- (23) Sousa, C.; Illas, F.; Pacchioni, G. *J. Chem. Phys.* **1993**, 99, 6818.
- (24) Pascual, J. L.; Seijo, S. *J. Chem. Phys.* **1995**, 102, 5368.
- (25) Seijo, L.; Barandiaran, Z. *J. Math. Chem.* **1992**, 10, 41.
- (26) Barandiaran, Z.; Seijo, L. In *Cluster Models for Surface and Bulk Phenomena*; Proceedings of the NATO ASI Series, Erice Sicily, 1991, Pacchioni, G., Bagus, P., Parmigiani, F., Eds.; Plenum: New York, 1992.
- (27) Mejias, J. A.; Fernandez-Sanz, J. *J. Chem. Phys.* **1995**, 102, 327.
- (28) Winter, N. W.; Pitzer, R. M.; *J. Chem. Phys.* **1988**, 89, 446.
- (29) Sugano, S.; Shuman, R. G. *Phys. Rev.* **1963**, 130, 517.
- (30) Richardson, J. W.; Vaught, D. M.; Soules, T. F.; Powell, R. R. *J. Chem. Phys.* **1972**, 5, 4291.
- (31) Pueyo, L.; Richardson, J. W. *J. Chem. Phys.* **1977**, 67, 3583.
- (32) Bagus, P. S.; Wahlgren, U. *Mol. Phys.* **1977**, 33, 541.
- (33) Barandiaran, Z.; Seijo, L. *J. Chem. Phys.* **1988**, 89, 5739.
- (34) Janssen, G. J. M.; Nieuwpoort, W. C. *Phys. Rev. B* **1988**, 38, 3449.
- (35) Bagus, P. S.; Illas, F.; Sousa, C. *J. Chem. Phys.* **1994**, 100, 2943.
- (36) Lorda, E.; Illas, F.; Bagus, P. S. *Chem. Phys. Lett.* **1996**, 256, 377.
- (37) Casanovas, J.; Illas, F. *J. Chem. Phys.* **1994**, 100, 8257.
- (38) Casanovas, J.; Rubio, J.; Illas, F. *Phys. Rev. B* **1996**, 53, 945.
- (39) Graaf, C.; Illas, F.; Broer, R.; Nieuwpoort, W. C. *J. Chem. Phys.* **1996**, 106, 3287.
- (40) Moreira, I. P. R.; Illas, F. *Phys. Rev. B* **1997**, 55, 4129.
- (41) Moore, C. E. *Atomic Energy Levels*; Natl. Bur. Stand. U.S. Circ. No. 467; GPO: Washington DC, 1952.
- (42) Hay, P. J.; Wadt, W. R. *J. Chem. Phys.* **1985**, 82, 299.
- (43) Broughton, J. Q.; Bagus, P. S. *Phys. Rev. B* **1984**, 30, 4761; **1987**, 36, 2813.
- (44) Huzinaga, S., Ed. *Gaussian Basis Sets for Molecular Calculations*; Physical Science Data 16; Elsevier: Amsterdam, 1984.
- (45) Becke, A. D. *Phys. Rev. A* **1988**, 38, 3098.
- (46) Lee, C.; Yang, W.; Parr R. G. *Phys. Rev. B* **1988**, 37, 785.
- (47) Colle, R.; Salvetti, O. *J. Chem. Phys.* **1983**, 79, 1404.
- (48) Balasubramanian, K. *J. Chem. Phys.* **1988**, 89, 6310.
- (49) Roos, B.; Siegbahn, P. *Theor. Chim. Acta* **1970**, 17, 199.
- (50) Becke, A. D. *J. Chem. Phys.* **1993**, 98, 5648.
- (51) Boys, S. F.; Bernardi, F. *Mol. Phys.* **1970**, 19, 553.
- (52) Frisch, M. J.; Trucks, G. W.; Schlegel, H. B.; Gill, P. M. W.; Johnson, B. G.; Robb, M. A.; Cheeseman, J. R.; Keith, T.; Petersson, G. A.; Montgomery, J. A.; Raghavachari, K.; Al-Laham, M. A.; Zakrzewski, V. G.; Ortiz, J. V.; Foresman, J. B.; Peng, C. Y.; Ayala, P. Y.; Chen, W.; Wong, M. W.; Andres, J. L.; Replogle, E. S.; Gomperts, R.; Martin, R. L.; Fox, D. J.; Binkley, J. S.; Defrees, D. J.; Baker, J.; Stewart, J. P.; Head-Gordon, M.; Gonzalez, C.; Pople, J. A. *Gaussian 94*, Revision B.3; Gaussian, Inc.: Pittsburgh, PA, 1995.
- (53) Luaña, V.; Recio, J. M.; Pueyo, L. *Phys. Rev. B* **1990**, 42, 1791.
- (54) Partridge, H. *Near Hartree-Fock Quality Gaussian Type Orbitals Basis Sets for the First and Third Row Atoms*; NASA technical memorandum 101044; 1989.
- (55) Rösch, N.; Pacchioni G. Private communication.
- (56) McLean, A. D.; Liu, B. *Chem. Phys. Lett.* **1983**, 101, 144.
- (57) Bauschlicher, C. W.; Taylor, P. R. *Theor. Chim. Acta* **1993**, 86, 13.
- (58) Delley, B. *J. Chem. Phys.* **1990**, 92, 508.
- (59) Henry, C. R.; Meunier, M.; Morel, S. *J. Crystal Growth* **1990**, 129, 416.
- (60) Bagus, P. S.; Pacchioni, G.; Philpott, M. R. *J. Chem. Phys.* **1989**, 90, 4287.
- (61) Bagus, P. S.; Illas, F. *Phys. Rev. B* **1990**, 42, 10852.
- (62) Baerends, E. J.; Branchadell, V.; Sodupe, M. *Chem. Phys. Lett.* **1997**, 265, 481.